

obeyika.com

LIST OF TABLES

List of Tables

Table(1):	Chemical composition of samples which used.....	33
Table(2):	Corrosion resistance and corrosion rate for L.C.V. steel samples at different concentrations of HNO ₃ at 25 °C.....	175
Table(3):	Corrosion resistance and corrosion rate for L.C.V. steel samples at different concentrations of HNO ₃ at 35 °C.....	176
Table(4):	Corrosion resistance and corrosion rate for L.C.V. steel samples at different concentrations of HNO ₃ at 45 °C.....	177
Table(5):	Corrosion resistance and corrosion rate for L.C.V. steel samples at different concentrations of HNO ₃ at 55 °C.....	178
Table(6):	Corrosion resistance and corrosion rate for L.C.V. steel samples at different concentrations of HEAA in 0.1 M HNO ₃ at 25 °C.....	179
Table(7):	Corrosion resistance and corrosion rate for L.C.V. steel samples at different concentrations of HEAA in 0.1 M HNO ₃ at 35 °C.....	180
Table(8):	Corrosion resistance and corrosion rate for L.C.V. steel samples at different concentrations of HEAA in 0.1 M HNO ₃ at 45 °C.....	181
Table(9):	Corrosion resistance and corrosion rate for L.C.V. steel samples at different concentrations of HEAA in 0.1 M HNO ₃ at 55 °C.....	182
Table(10):	Corrosion resistance and corrosion rate for M.C.V. steel samples at different concentrations of HNO ₃ at 25 °C.....	183
Table(11):	Corrosion resistance and corrosion rate for M.C.V. steel samples at different concentrations of HNO ₃ at 35 °C.....	184
Table(12):	Corrosion resistance and corrosion rate for M.C.V. steel samples at different concentrations of HNO ₃ at 45 °C.....	185
Table(13):	Corrosion resistance and corrosion rate for M.C.V. steel samples at different concentrations of HNO ₃ at 55 °C.....	186
Table(14):	Corrosion resistance and corrosion rate for M.C.V. steel samples at different concentrations of HEAA in 0.1 M HNO ₃ at 25 °C.....	187
Table(15):	Corrosion resistance and corrosion rate for M.C.V. steel samples at different concentrations of HEAA in 0.1 M HNO ₃ at 35 °C.....	188

Table(16): Corrosion resistance and corrosion rate for M.C.V. steel samples at different concentrations of HEAA in 0.1 M HNO ₃ at 45 °C.....	189
Table(17): Corrosion resistance and corrosion rate for M.C.V. steel samples at different concentrations of HEAA in 0.1 M HNO ₃ at 55 °C.....	190
Table(18): Inhibition efficiency of different concentrations of HEAA in 0.1M HNO ₃ for as cast L.C.V. steel sample at various temperatures.	209
Table(19): Inhibition efficiency of different concentration of HEAA in 0.1M HNO ₃ for normalized L.C.V. steel sample at various temperatures.....	210
Table(20): Inhibition efficiency of different concentrations of HEAA in 0.1M HNO ₃ for spheroidized L.C.V. steel sample at various temperatures.	211
Table(21): Inhibition efficiency of different concentrations of HEAA in 0.1M HNO ₃ for quenched L.C.V. steel sample at various temperatures.	212
Table(22): Inhibition efficiency of different concentration of HEAA in 0.1M HNO ₃ for as cast M.C.V. steel sample at various temperatures.	213
Table(23): Inhibition efficiency of different concentrations of HEAA in 0.1M HNO ₃ for normalized M.C.V. steel sample at various temperatures.....	214
Table(24): Inhibition efficiency of different concentrations of HEAA in 0.1M HNO ₃ for spheroidized M.C.V. steel sample at various temperatures.	215
Table(25): Inhibition efficiency of different concentrations of HEAA in 0.1M HNO ₃ for quenched M.C.V. steel sample at various temperatures.....	216
Table(26): Activation energy of L.C.V. steel samples in 0.1MHNO ₃ and absence of inhibitor HEAA at various temperature.....	225
Table(27): Activation energy of L.C.V. steel samples in 0.1M HNO ₃ in 2x10 ⁻⁵ M of inhibitor HEAA at various temperature.....	226
Table(28): Activation energy of L.C.V. steel samples in 0.1M HNO ₃ in 4x10 ⁻⁵ M of inhibitor HEAA at various temperature.....	227
Table(29): Activation energy of L.C.V. steel samples in 0.1M HNO ₃ in 6x10 ⁻⁵ M of inhibitor HEAA at various temperature.....	228
Table(30): Activation energy of L.C.V. steel samples in 0.1M HNO ₃ in 8x10 ⁻⁵ M of inhibitor HEAA at various temperatures.....	229

Table(31): Activation energy of L.C.V. steel samples in 0.1M HNO ₃ in 10 ⁻⁴ M of inhibitor HEAA at various temperature.	230
Table(32): Activation energy of M.C.V. steel samples in 0.1MHNO ₃ and absence of inhibitor HEAA at various temperature.....	231
Table(33): Activation energy of M.C.V. steel samples in 0.1M HNO ₃ in 2x10 ⁻⁵ M of inhibitor HEAA at various temperature.....	232
Table(34): Activation energy of M.C.V. steel samples in 0.1M HNO ₃ in 4x10 ⁻⁵ M of inhibitor HEAA at various temperature.....	233
Table(35): Activation energy M.C.V. steel samples in 0.1M HNO ₃ in 6x10 ⁻⁵ M of inhibitor HEAA at various temperature.....	234
Table(36): Activation energy of M.C.V. steel samples in 0.1M HNO ₃ in 8x10 ⁻⁵ M of inhibitor HEAA at various temperature.....	235
Table(37): Activation energy of M.C.V. steel samples in 0.1M HNO ₃ in 10 ⁻⁴ M of inhibitor HEAA at various temperature.....	236
Table(38): Calculation of binding constant (K)of HEAA in langmuir equation in 0.1M HNO ₃ for as cast L.C.V. steel sample at various temperatures.....	241
Table(39): Calculation of binding constant (K)of HEAA in langmuir equation in 0.1M HNO ₃ for normalized L.C.V. steel sample at various temperatures.....	242
Table(40): Calculation of binding constant (K)of HEAA in langmuir equation in 0.1M HNO ₃ for spheroidized L.C.V. steel sample at various temperatures.....	243
Table(41): Calculation of binding constant (K)of HEAA in langmuir equation in 0.1M HNO ₃ for quenched L.C.V. steel sample at various temperatures.....	244
Table(42): Thermodynamic parameters of adsorption-desorption process for L.C.V. steel samples in 0.1M HNO ₃ in presence of different concentration of HEAA Calculated from equilibrium constant of langmuir equation.....	245
Table(43): Calculation of binding constant (K)of HEAA in langmuir equation in 0.1M HNO ₃ for as cast M.C.V. steel sample at various temperatures.....	250
Table(44): Calculation of binding constant (K)of HEAA in langmuir equation in 0.1M HNO ₃ for normalized M.C.V. steel sample at various temperatures.....	251
Table(45): Calculation of binding constant (K)of HEAA in langmuir equation in 0.1M HNO ₃ for spheroidized M.C.V. steel sample at various temperatures.	252

Table(46): Calculation of binding constant (K)of HEAA in langmuir equation in 0.1M HNO₃ for quenched M.C.V. steel sample at various temperatures.....	253
Table(47): Thermodynamic parameters of adsorption-desorption process for M.C.V. steel samples in 0.1M HNO₃ in presence of different concentration of HEAA Calculated from equilibrium constant of langmuir equation.....	254
Table(48): Calculation of binding constant (K)of HEAA in frumkin equation in 0.1M HNO₃ for as cast L.C.V. steel sample at various temperatures.....	259
Table(49): Calculation of binding constant (K)of HEAA in frumkin equation in 0.1M HNO₃ for normalized L.C.V. steel sample at various temperatures.....	260
Table(50): Calculation of binding constant (K)of HEAA in frumkin equation in 0.1M HNO₃ for spheroidized L.C.V. steel sample at various temperatures.....	261
Table(51): Calculation of binding constant (K)of HEAA in frumkin equation in 0.1M HNO₃ for quenched L.C.V. steel sample at various temperatures.....	262
Table(52): Thermodynamic parameters of adsorption-desorption process for L.C.V. steel samples in 0.1M HNO₃ in presence of different concentration of HEAA Calculated from equilibrium constant of frumkin equation.	263
Table(53): Calculation of binding constant (K)of HEAA in frumkin equation in 0.1M HNO₃ for as cast M.C.V. steel sample at various temperatures.....	268
Table(54): Calculation of binding constant (K)of HEAA in frumkin equation in 0.1M HNO₃ for normalized M.C.V. steel sample at various temperatures.....	269
Table(55): Calculation of binding constant (K)of HEAA in frumkin equation in 0.1M HNO₃ for spheroidized M.C.V. steel sample at various temperatures.....	270
Table(56): Calculation of binding constant (K)of HEAA in frumkin equation in 0.1M HNO₃ for quenched M.C.V. steel sample at various temperatures.....	271
Table(57): Thermodynamic parameters of adsorption-desorption process for M.C.V. steel samples in 0.1M HNO₃ in presence of different concentration of HEAA Calculated from equilibrium constant of frumkin equation.....	272

Table(58): Data of El-Awady thermodynamic model application for as cast L.C.V. steel sample in 0.1M HNO ₃ in presence of different concentration of HEAA at various temperatures..	277
Table(59): Data of El-Awady thermodynamic model application for normalized L.C.V. steel sample in 0.1M HNO ₃ in presence of different concentration of HEAA at various temperatures.....	278
Table(60): Data of El-Awady thermodynamic model application for spheroidized L.C.V. steel sample in 0.1M HNO ₃ in presence of different concentration of HEAA at various temperatures.	279
Table(61): Data of El-Awady thermodynamic model application for quenched L.C.V. steel sample in 0.1M HNO ₃ in presence of different concentration of HEAA at various temperatures..	280
Table(62): Thermodynamic parameters of adsorption-desorption process for L.C.V. steel samples in 0.1M HNO ₃ in presence of different concentration of HEAA Calculated from equilibrium constant of El-Awady equation.	281
Table(63): Data of El-Awady thermodynamic model application for as cast M.C.V. steel sample in 0.1M HNO ₃ in presence of different concentration of HEAA at various temperatures..	286
Table(64): Data of El-Awady thermodynamic model application for normalized M.C.V. steel sample in 0.1M HNO ₃ in presence of different concentration of HEAA at various temperatures.....	287
Table(65): Data of El-Awady thermodynamic model application for spheroidized M.C.V. steel sample in 0.1M HNO ₃ in presence of different concentration of HEAA at various temperatures.	288
Table(66): Data of El-Awady thermodynamic model application for quenched M.C.V. steel sample in 0.1M HNO ₃ in presence of different concentration of HEAA at various temperatures.....	289
Table(67): Thermodynamic parameters of adsorption-desorption process for M.C.V. steel samples in 0.1M HNO ₃ in presence of different concentration of HEAA Calculated from equilibrium constant of El-Awady equation.....	290

o
b
e
i
k
n
g
r
e
t
i
c
o
m

ENGLISH SUMMERY

Summary

Low and medium carbon vanadium steel (L.C.V and M.C.V respectively) are two types of reinforcement steel, which used in construction of concrete pipes in sanitary pipelines. Different heat treatment regimes would be applied to obtain suitable required mechanical properties. Spheroidizing regime would be used for high ductility of steel, and normalizing regime for a partially increasing of tensile strength, otherwise quenching for obtaining the highest tensile strength.

Acidic waste were attacking steel in side concrete by corrosion, then some organic or inorganic corrosion inhibitors would be mixed with fresh concrete during concrete's pouring to protect steel inside concrete against corrosion.

HNO₃ acid would be used in this work as acid media with different concentration(0.1, 0.3 and 0.5M) at various temperature(25, 35, 45 and 55°C) in absence of inhibitor and 0.1M of HNO₃ acid only was used with different concentrations of HEAA (N,N di hydroxyethyl acrylamid) as a corrosion inhibitor (2×10^{-5} , 4×10^{-5} , 6×10^{-5} , 8×10^{-5} and 10^{-4} M) at the same various temperatures.

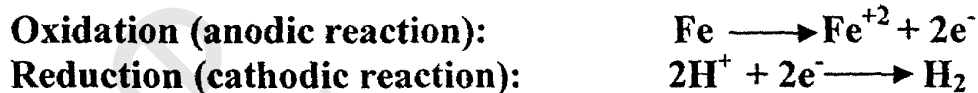
The corrosion rates were measured by polarization technique. Microstructure of all C.V. steel samples and micrographs were investigated by microscopic inspection, and photography.

1-Corrosion behavior in HNO₃

By inspection of the corrosion rate data it is obvious to observe that the corrosion rates of all samples of C.V.steel are increasing with increasing of concentration of HNO₃ in the order $0.5 > 0.3 > 0.1$ M, as a result of increasing of H⁺ concentration (cathodic reactant).

2-Effect of temperature on corrosion behavior

The corrosion rate data illustrate that the rate of corrosion increases with increasing the temperature as following order: $25^{\circ}\text{C} < 35^{\circ}\text{C} < 45^{\circ}\text{C} < 55^{\circ}\text{C}$ for all C.V steel samples as a result of decreasing the apparent activation energy E^* of the charge transfer reaction.



The increase in temperature will enhance the rate of H^{+} diffusion to the metal surface as well as ionic mobility . At lower temperature the adsorbed hydrogen atoms block the cathodic area, while the increase in the solution temperature causes desorption of hydrogen, Such hydrogen desorption leading to the increase of cathodic area and consequently increase the corrosion rate.

In general, all the previous corrosion rate data for L.C.V. and M.C.V. steel samples whether in absence or presence of HEAA as inhibitor show that the most predominant order in the corrosion rate decreases as follows

$$A > Q > N > S$$

(with exception at 45 and 55 °C)

where (A: as-received, Q: quenched, N: normalized, S: spheroidized)

In the light of this general order, its obvious that any heat treatment regime alike the employed in these study resist the corrosion processes.

It worth-note that the corrosion rate of L.C.V.steel samples were much more higher than for M.C.V.steel samples whether in presence and absence of the inhibitor (but at very few cases of 45 and 55°C the corrosion rate of M.C.V steel samples were higher than L.C.V steel samples). Then, in other word, one can say that M.C.V.steel resists the corrosion more than L.C.V.steel. This is may be interpreted from the lower percentage of ferrite phase in M.C.V.steel than that for L.C.V.steel.

3-Effect of inhibitor(HEAA) on corrosion behavior

The inhibition efficiency(P%) can be calculated from the following equation:

$$P\% = (r - r')/r \times 100$$

Where r and r' are the corrosion rate in absence and presence of inhibitor.

Inspection the inhibition efficiency data it will be clear that this inhibition efficiency for all samples under study increases with increasing HEAA in the used concentration rang as follows:

$$10^{-4} > 8 \times 10^{-5} > 6 \times 10^{-5} > 4 \times 10^{-5} > 2 \times 10^{-5} \text{ M HEAA}$$

And obvious that the higher inhibition efficiency was observed mostly in quenched heat treated. Then it was concluded that the martensitic surfaces (of L.C.V. or M.C.V.steel samples) are the best suitable surface using HEAA as inhibitor in 0.1 M HNO₃. In general, the inhibition efficiency decreases by increasing temperature in case of 25,45, and 55 °C (taking account an abnormal of inhibition efficiency at 35 °C which has a lower values than those at the other temperature). This above behavior indicates that the inhibitor HEAA molecules controlled by inhibition mechanism and can be described as complex formation on the metal surface , but at high temperature(45, 55°C) this complex is decomposition.

Single S-shape were obtained from plotting inhibition efficiency(P%) versus logarithm of concentration of HEAA (log [I]) in 0.1 M HNO₃ . This means the formation of one layer from HEAA molecules over the metal surfaces in all cases under study.

4- Activation energy (E*)

The activation energy E* for the corrosion rates were calculated from Arrheniuse.type equation:

$$\ln r = \ln A - E^*/RT$$

where r = corrosion rate

A = Arrhenius pre exponential factor

R = ideal gas constant

T = absolute temperature.

Plotting $\ln r$ vs. $1/T$ and E^* would be deduced from slope $= -E^*/2.303R$.

Values of E^* for all samples in presence and absence of different concentrations of HEAA are indicating that:

1. In case of L.C.V. steel samples the activation energy values of the normalizing samples in presence and absence of the inhibitor are higher than those of the other samples. Also, the activation energy values of the normalizing sample in presence of the inhibitor are higher than those in absence of the inhibitor.
2. In case of M.C.V. steel samples, the activation energy values of the quenched sample is higher than those for other samples in absence of the inhibitor. While in case of presence of the inhibitor the activation energy values of the normalizing sample are higher than those of the other samples.

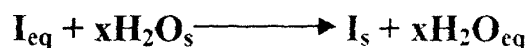
This attributed to that these heat treatments for these samples may be increase the energy barrier of the activation processes.

5- Thermodynamic parameters of adsorption processes

Three models of surface chemistry were used to investigate corrosion inhibition mechanism of HEAA adsorption on the metal surfaces. The above models which used in this work are Langmuir, Frumkin and El-Awady.

Molecules of HEAA inhibit the corrosion process by adsorption on metal surface. Theoretically, the adsorption process can be regarded as a single substitutional process in which an inhibitor molecule in the aqueous phase

substitutes an (x) number of water molecules adsorbed on the metal surface as in the following equation:



Where (x) is known as the size ratio and is simply equal to the number of adsorbed water molecules replaced by a single inhibitor molecule. The adsorption depends on the structure of the inhibitor, the type of the metal and the nature of its surface, the nature of the corrosion medium and its pH value and temperature.

A) Langmuir isotherm

Langmuir's equation can be written as follows:

$$\theta/1-\theta = K[I]$$

Where K is equilibrium constant of the adsorption reaction,
 $[I]$ is concentration of HEAA in the bulk of the solution,
 θ is the surface coverage, which can be calculated from the following equation:

$$\theta = 1 - (r/r)$$

Where r and r are the corrosion rate in the presence and absence of inhibitor respectively. K 's values can be obtained by plotting $\theta/1-\theta$ against $[I]$, all curves of Langmuir are straight lines indicating the validity of applying the Langmuir model. Thermodynamic parameters of the adsorption process were calculated from the following equation:

$$\Delta G^\circ = -2.303 RT \log K$$

$$\Delta S^\circ = \frac{\Delta H^\circ - \Delta G^\circ}{T}$$

Where ΔG° , ΔH° and ΔS° are standard free energy, enthalpy and entropy changes respectively. It is obviously described to obtain the standard enthalpy (ΔH°) by the study of the binding constant (K) over temperature range by applying a linear-least squares analysis according to the Van't Hoff's isochore.

$$\frac{d(\ln K)}{d(T^{-1})} = \frac{-\Delta H^\circ}{R}$$

or

$$\ln K = \frac{-\Delta H^\circ}{RT} + \frac{\Delta S^\circ}{R}$$

Where the values of $\log K$ are plotted versus T^{-1} giving a straight line with slope equal to $(-\Delta H^\circ/2.303 R)$. Hence, the standard enthalpy changes ΔH° can be evaluated.

All ΔG° values for all samples under study are negative at different temperatures indicating to spontaneously of adsorption processes. But ΔH° values for all samples under study are positive referring to endothermicity of the adsorption processes. This behavior supported by the binding constant values which increases as the temperature increases indicating that the adsorption processes are endothermic ones which agree with the positive values of the standard enthalpy changes, Also, the spontaneity increases with increasing temperature as a result of the increasing the negativity ΔG° with increasing the temperature. The positive values of ΔS° indicate that these adsorption processes are entropy favored processes, where the positive ΔS° values are applicable with the negative ΔG° .

B) Frumkin isotherm

The second thermo dynamic model is Frumkin's equation which could be written as follows:

$$\ln\left\{\frac{\theta}{1-\theta}\right\} = \ln K + 2a\theta$$

Where "a" = Lateral inter action term between adsorbed molecules describing the interaction in the adsorbed area and the measurement of steepness of the adsorption. Other terms in the equation are as mentioned above.

Most values of "a" are negative values or less than unity indicating a weak adsorption of HEAA molecules except in few cases, the values of "a" near or more than unity indicating strong adsorption of HEAA molecules in

such few cases. A plot of $\ln\{\theta/(1-\theta) [I]\}$ against θ gives a curvature relationship (not a straight line) indicating to Invalidity of Frumkin model. In this case, the values of K as well as (a) were calculated by using least square fit.

All ΔG° values are negative denoting that adsorption process proceeds spontaneously. In case of L.C.V.steel samples, all (ΔH°) values have negative values indicating to exothermicity of the adsorption processes of HEAA molecules, the negative values of ΔS° in this case indicating that these adsorption processes were enthalpy favored processes. Similar were observed in case of M.C.V.steel samples of MN and MS, while in case of MA and MQ samples the adsorption processes were entropy favored processes where ΔS° and ΔH° have a positive values.

C) El-Awady isotherm

El-Awady equation was modified to the following one:

$$\log \theta/(1-\theta) = x \log K + 1/x \log [I]$$

Where “x” = Number of sites on the metal surface which can be replaced by one molecule of the inhibitor. “x” Values are near or more than unity indicating a strong adsorption of inhibitor molecules on the metal surface. Straight lines of plotting $\log \theta/(1-\theta)$ against $\log [I]$ are indicating to the validity of modified model of El-Awady. All ΔG° values are negative indicating to spontaneously of adsorption processes. ΔH° values are positive in most cases indicating to endothermicity of the adsorption processes, while negative in case of MS sample due to exothermic nature of this adsorption process. Also, the K values increase as the temperature increases in most cases.

The positive ΔS° values indicate the disordered adsorption processes of HEAA molecules over the metal surfaces. These positive values of ΔS° applicable with the negative ΔG° values indicate that the adsorption processes in these cases are entropy favored processes.

From values of ΔG° , ΔH° , and ΔS° in above three models it is obvious that the adsorption processes are mixed (physical and chemical) adsorption.

On comparison of the present data of the three models, it is obvious that the validity of the Langmuir isotherm and of El-Awady isotherm due to their obtained straight lines, while the application of Frumkin thermodynamic model yields a curvature isotherm, this curvature isotherm as well as the negative "a" values indicating the invalidity of the Frumkin model if compared with Langmuir isotherm and El-Awady isotherm.

Although there is very good agreement between Langmuir isotherm and El-Awady model in the thermodynamic parameters and the binding constant behavior, it was concluded that the best applied thermodynamic model for the adsorption of HEAA molecules on various surface of the studied metal is Langmuir adsorption isotherm.

This final conclusion due to the excellent obtained straight line in application of Langmuir isotherm than that obtained from El-Awady.